Pergamon

Journal of Structural Geology, Vol. 16, No. 6, pp. 867 to 881, 1994

0191-8141/94 $07.00 + 0.00

Dynamic recrystallization of quartz under greenschist conditions

GEOFFREY E. LLOYD

Department of Earth Sciences, The University, Leeds LS2 9JT, U.K.

and

BRETT FREEMAN

Badley Earth Sciences, Winceby House, Winceby, Horncastle, Lincolnshire LN9 6PB, U.K.

(*Received* 26 *October* 1992; *accepted in revised form* 15 *July* 1993)

Abstract—The SEM electron channelling technique has been used to investigate the dynamic recrystallization of three quartz grains representative of optical textures observed in quartzite deformed under greenschist facies conditions. The degree of recrystallization has been determined at 10–20, ~50 and 100%, respectively. We demonstrate that dynamic recrystallization is a sequential process involving subgrain–grain rotation and grain-boundary migration. It initiates via subgrain polygonization on a single crystal slip system, and continues via subgrain and neoblast rotation on several slip systems. In the early stages of recrystallization (< 50%), the orientation relationships between subgrains–neoblasts and parent grains are systematic and are related to the dominantly active crystal slip systems. Beyond ~50% recrystallization, orientation relationships are less systematic and this is attributed to an increase in the activity of grain-boundary migration. However, dynamic recrystallization is potentially a cyclical process with new subgrains forming within migrational neoblasts due to continued deformation. The three sequences represent different stages in the same continuous, time- or strain-dependent, dynamic recrystallization history. They therefore combine to give a generalized dynamic recrystallization history for greenschist facies quartz grains at low to moderate strains. Porphyroclasts have similar recrystallization histories because the original bimodal grain size distribution leads to strain partitioning, allowing the porphyroclasts to rotate into weak orientations with the subsequent activation of weak crystal slip systems.

INTRODUCTION: DYNAMIC RECRYSTALLIZATION

DYNAMIC recrystallization occurs during deformation (e.g. Poirier & Guillope 1979) and involves the establishment of an array of grain boundaries in new material positions (Means 1983) and the formation and/or migration of grain boundaries (Vernon 1981). These processes operate in order to minimize strain energy. The definition of dynamic recrystallization depends on the scale of the observation. Urai *et al.* (1986) suggest that at the scale of a grain boundary all dynamic recrystallization in silicates takes the form of grain-boundary migration, achieved by the mobility of atoms. This conforms with the metallurgical interpretation of dynamic recrystallization (e.g. Cahn 1965). However, despite a large and widespread effort, the physical nature of grain boundaries in geological materials remains unclear (White & White 1981, McClaren 1986, Hay & Evans 1988), which prevents, for the moment, the adoption of the metallurgical approach by earth scientists.

At the grain scale, dynamic recrystallization produces two characteristic crystallographic textures which are interpreted to represent two distinct processes: (1) progressive misorientation of subgrains; and (2) grain-boundary migration. However, both processes often result in similar microstructures, leading to misinterpretation. There is also a danger of misinterpretation between real dynamic recrystallization and similar optical microstructures which are now known to be produced by fracturing and kinking (Urai *et al.* 1986). The importance of the latter cannot be overstated since most microstructural investigations are performed at the grain scale.

Some authors have suggested that the full range of phenomena observed at the grain scale is not adequately described by a two-fold categorization (Urai *et al.* 1986, Drury & Urai 1990) and that there are four characteristic microstructures, which imply four distinct processes. These processes are, respectively (Drury *et al.* 1985): (1) subgrain rotation; (2) subgrain growth; (3) grain-boundary bulging; and (4) grain growth. Items (2), (3) and (4) effectively represent a superset of the migration recrystallization end-member and although they may be recognizable in experimental studies, their practical use in the description of rock textures and microstructures is somewhat limited.

Grain-boundary migration

During grain-boundary migration the internal elastic strain due to unbound dislocations is relaxed as the strained grain is 'consumed' by a neighbouring, relatively strain free, grain(s). The intervening grain boundary sweeps across the deformed lattice leaving reordered and strain-free crystal structure in its wake. There is some evidence to suggest that this process may

be assisted by the presence of a grain-boundary fluid (Ohtomo & Wakahama 1982, 1983, Toriumi 1982, Urai 1983, 1985). Grain-boundary migration is generally a conservative process, although material may be lost or gained where it is associated with diffusive mass transfer. The direction of migration of boundaries is away from their centre of curvature. This leads to a distinctive microstructure because initially straight boundaries become lobate or sutured, and often show a tendency to bulge (e.g. Etheridge & Hobbs 1974, Vernon 1975, 1981, Avé L'Allement 1978, McClay & Atkinson 1977; see also Hirth & Tullis 1992). One of the implications following the concept of grain-boundary migration is that the physical manifestation of a grain is only temporarily associated with its material points (e.g. Means 1989).

The velocity of grain-boundary migration (v_{gbm}) is influenced by the relative crystallographic characteristics of adjacent grains, the driving force(s), temperature and the structure of the boundary. Crystallography exerts a complex influence and several orders of magnitude increase in v_{gbm} can occur as the mismatch between adjacent grains increases (Haessner & Hoffman 1978). Furthermore, orientation differences between adjacent grains have a primary effect on relative deformation rates and hence dislocation densities, which leads to a secondary effect on v_{gbm} rates. Driving forces include lattice defects, grain-boundary energy, chemical free energy and external elastic energy, and always lead to a decrease in internal strain energy.

It has been shown for metals that v_{gbm} has a first-order rate dependency on temperature (Haessner & Hoffman 1978, Guillope & Poirier 1979) and a similar relationship is expected for minerals. At relatively high homologous temperatures, migration will dominate any microstructure, even during deformation (e.g. Jessell 1986, Means & Jessell 1986, Means & Ree 1988, Bons & Urai 1992). This is also the situation which exists in metamorphic aureoles, particularly close to the igneous contact, during both dynamic and static (annealing) recrystallization conditions (e.g. Joesten 1983).

The structure of the boundaries includes whether they contain a fluid phase ('dry' or 'wet' boundaries) and the presence or absence of impurities. Migration rates are potentially enhanced by the presence of a fluid phase, whilst the presence of impurities (whatever the scale) can seriously retard grain-boundary migration (see discussion in Hay & Evans 1988, for details).

Subgrain rotation

The microstructures typical of subgrain rotation dynamic recrystallization are the so-called 'core-and-mantle' structure (Gifkins 1976, White 1976) and, particularly where recrystallization is complete, clusters of grains with similar orientations. Grain-boundary triple junctions and/or 120° dihedral angles are rare, in the absence of grain-boundary migration.

There is little documentation on the actual processes involved in subgrain rotation, but these are likely to include: accommodation of misorientation across boundaries (by some degree of subgrain and grain-boundary migrations); deformation and strain compatibility (Cobbold *et al.* 1984); and the influence of external loads. Thus, the controls on, and velocity (v_{rm}) of, rotational subgrain boundary dynamic recrystallization are much less understood than for migration. However, we know that crystal structure must influence the ability of a grain to form subgrains because it controls directly the propensity of a grain to undergo heterogeneous deformation.

Observations show that during subgrain rotation new grains or neoblasts evolve by the addition of dislocations of predominantly one sign into an existing subgrain wall. This produces relative rotation of the lattice on either side of the subgrain wall and eventually leads to the development of a high-angle grain boundary (e.g. Garofalo *et al.* 1961, Poirier & Nicolas 1975). The misorientation needed to establish a new grain during rotational recrystallization is largely a matter for definition because published values depend on the method and precision of observation. Suggested values range from 1° to 15° (e.g. Poirier & Nicolas 1975, Guillope & Poirier 1979, Fitzgerald *et al.* 1983), usually measured relative to a specific crystal direction (e.g. quartz *c*-axis via optical microscopy) and may therefore ignore or dismiss alignments of other crystal directions which are not readily determinable (e.g. quartz *a*-axes).

We propose that a more pragmatic definition of a 'new' grain (resulting from rotation recrystallization) corresponds to a threshold misorientation at which boundary migration may occur for the given temperature. Thus, we expect high misorientations and marked rotation microstructures at low homologous temperatures, and low misorientations and a much diminished, relatively, rotation free microstructure at high homologous temperatures. This is consistent with the observations of Hirth & Tullis (1992), who note the tendency of subgrain rotation to be favoured by high deviatoric stresses and low temperature.

Distinction between migration and rotation

An essential difference between the two basic dynamic recrystallization processes becomes obvious if we consider the behaviour of a single porphyroclast. For migration, the newly formed grains within the original porphyroclast grain boundary will have their crystallographic orientations controlled by the neighbouring grains. Thus, the new grains represent a sample from the bulk fabric. Conversely, for rotation, the newly formed grains are derived from the porphyroclast and hence their crystallographic orientation will depend on the orientation of their host (e.g. Poirier & Nicolas 1975). Normally, this subfabric does not have a simple relationship to the bulk fabric, although it should contain information on the specific slip systems active during deformation.

In order to understand how these two fundamentally different processes co-operate requires a complete crys-

tallographic description, combined with a spatial description, of the porphyroclast, new subgrains and neoblasts, and neighbouring grains. Due to technical limitations, this is not possible with conventional techniques (e.g. optical microscopes fitted with a universal stage, transmission electron microscopy, X-ray texture goniometry). However, all the required data are accessible using the scanning electron microscope (SEM) operated in the electron channelling (EC) mode (Joy *et al.* 1982, Lloyd 1987, Lloyd *et al.* 1991, 1992).

SAMPLE AND ANALYTICAL DETAILS

Sample location

In this study we are concerned only with the dynamic recrystallization of quartz grains in relatively pure quartzites (see also Hobbs 1968, Tullis *et al.* 1973, Hirth & Tullis 1992), which represent a relatively simple geological system. The sample studied comes from a relatively pure quartzite bed in the Crinan Grits of the Argyll Group, Dalradian Supergroup, southwest Highlands of Scotland. Its structural position is in the limb between the NW syncline and the Cnoc Stigsheir anticline (U.K. Ordinance Survey grid reference NR 712768), which comprise part of the major Kilmory Bay syncline (Freeman 1985). Although elsewhere in the southwest Highlands deformation is clearly polyphase, this fold is a primary structure which is largely unaffected by subsequent (i.e. post-D_1) disturbances (Roberts 1977, Freeman 1985). The presence of chlorite in cleavage fabrics and actinolite in the nearby metagabbro intrusives indicate syn-deformational greenschist facies metamorphism. Oxygen isotope geothermometry (Kerrich *et al.* 1977) suggests temperatures of 370–400°C.

Many beds within the Crinan Grits contain slightly carbonate-rich concretions which have near perfect elliptical outlines on flat planar sections. The lack of cleavage refraction about these concretions indicates that in spite of the compositional difference between them and the surrounding rock, they nevertheless behaved approximately as passive markers during deformation. Furthermore, their consistently similar axial ratios and parallelism with cleavage on nearly all sections indicates that they were probably almost spherical before deformation. These concretions therefore make ideal strain markers and at the sample locality the axial ratio of the strain ellipse determined from concretion measurements made on a single outcrop plane is 4.7:1 (Freeman 1984, 1985). We take this to be a minimum value for the XZ section through the strain ellipsoid (where $X \geqslant Y \geqslant Z$).

Sample description

Thin-sections were made from the sample parallel to all three principal planes of the strain ellipsoid. However, in this study we confine our attention to a single 30 μm thick thin-section cut parallel to the XZ section. Unlike transmission electron microscopy, the electron beam does not usually damage the specimen during SEM analysis, and hence the same specimen can be examined repeatedly using both SEM and optical techniques. We have used conventional optical microscopy to describe the bulk rock texture and strain homogeneity in the sample considered. These observations are summarized as follows.

Quartz grain sizes are bimodally distributed between a small size fraction ($\leqslant 50$ μm) consisting of matrix and recrystallized grains, and a large size fraction ($\leqslant 1000$ μm) consisting of porphyroclasts. To some extent, the porphyroclasts retain their original rounded sedimentary character (e.g. Lloyd & Freeman 1991a, fig. 1a; compare also Fig. 1a in this paper). Those which have suffered little or no recrystallization define a weak dimensional preferred orientation (DPO) parallel with cleavage. Matrix grains are polygonal and have no DPO. Boundaries between grains are either straight or slightly bowed with occasional bulges. We interpret these as incipient grain-boundary migration textures. Grain and high-angle subgrain boundaries are often decorated with fluid inclusions. There is a predominance of four (and higher) grain point contacts over triple point contacts, which implies that microstructural equilibrium has not been reached.

Impurities are present in the microstructure in the form of accessory feldspars, micas (muscovite and chlorite) and rutile. The micas fall into three morphological groups: (1) small, evenly spaced sub-euhedral laths with a slight DPO parallel to the bulk extension direction; (2) semi-continuous seams, usually only one crystal in width, which form an anastomosing pattern controlled by the location and size of the quartz porphyroclasts—these define the rock cleavage seen at outcrop and hand-specimen scales; and (3) dispersed ragged clumps in the strain shadows of detrital or recrystallized porphyroclasts. Dark field illumination shows that many of the quartz porphyroclasts contain abundant rutile inclusions. Freeman (1984) has shown how these inclusions permit calculation of the degree of dynamic recrystallization. In this specimen we find that $\sim 12\%$ of the total rock volume consists of new grains dynamically recrystallized from porphyroclasts and that the volume of porphyroclasts has been reduced by $\sim 37\%$.

Two independent methods of strain analysis show that deformation is heterogeneous between porphyroclasts and matrix. First, rutile inclusion orientation distributions (approximately von Mises) have a variability which can only be explained by heterogeneous strain (Freeman 1985). The distributions have been characterized by their 'β_2-values' (a statistical index which describes the fourth sample moment, or kurtosis, of the distribution; see Lloyd 1983, for details). These indicate a minimum 'porphyroclast-equals-dislocation-creep' strain of between 1.4 and 2.8 (Freeman 1985). Second, R_f/ϕ measurements made from the pre-recrystallization grain boundary shapes and orientations of porphyro-

Table 1. Predicted orientations of crystal directions due to rotational dynamic recrystallization on specific crystal slip systems (e.g. Figs. 3c and 4c).

	Crystal slip systems						
Pole	Basal-*a*	Basal-*m*	Basal prism	Positive rhomb-*a*	Negative rhomb-*a*	Positive acute rhomb-*a*	Negative acute rhomb-*a*
c	great circle through *a* slip pole	great circle through *m* slip pole	cluster parallel to rotation axis	37/143° small circle	37/143° small circle	52/128° small circle	52/128° small circle
m	rotation axis cluster; 60/120° small circle	great circle through *m* slip pole; 30/150° small circle	great circle through basal plane	53/127° and 72/108° small circles	53/127° and 72/108° small circles	37/143° and 67/113° small circles	37/143° and 67/113° small circles
a	great circle through *a* slip pole 30/150° small circle	rotation axis cluster; 60/120° small circle	great circle through basal plane	58/122° small circle; great circle through slip pole	58/122° small circle; great circle through slip pole	47/133° small circle; great circle through slip pole	47/133° small circle; great circle through slip pole
r	33/147° and 66/114° small circles	44/136° small circle; rotation axis normal great circle	57/123° small circle	47/133° and 85/95° small circles	19/161° and 80/100° small circles	70/110° and 49/131° small circles	5/175° small circle; great circle through slip pole
z	33/147° and 66/114° small circles	44/136° small circle; rotation axis normal great circle	57/123° small circle	19/161° and 80/100° small circles	47/133° and 85/95° small circles	5/175° circle; great circle through slip pole	70/110° and 49/131° small circles

clasts define patterns which do not satisfy a heterogeneous strain model because the implied strain ratio is inconsistent with the position of the 50% of data curve (Freeman 1985).

Analytical procedures

In this study, we augment the observations of Lloyd & Freeman (1991a) on Grain B with observations on two other grains from the same thin-section: Grain A, 10–20% dynamically recrystallized; and Grain C, 100% dynamically recrystallized. We can be certain of the parentage of all subgrains and most neoblasts in this specimen (whether via rotation or migration processes) because the original grain dimensions and positions have been determined from rutile inclusions (Freeman 1984, 1985). Our principal aim is to distinguish the specific dynamic recrystallization process(es) which have occurred. Thus, we look closely at subgrain and neoblast orientations with respect to their parent grain and also the parent grain's absolute orientation in terms of the bulk finite strain ellipsoid. We should therefore be able to define individual dynamic recrystallization histories for the grains under scrutiny, from which it is possible to make predictions about the dynamic recrystallization history for other grains in the specimen.

We adopt the same approach described by Lloyd & Freeman (1991a,b), using the advantages offered by the SEM–EC technique and the computer-aided indexing program *CHANNEL* (Schmidt & Olesen 1989). Lloyd & Freeman (1991a,b) used SEM–EC to compare crystal pole-figure diagrams for an individual quartz porphyroclast (Grain B, ~50% dynamically recrystallized) with theoretical crystal direction dispersion paths for individual crystal slip systems. Changes in crystal orientation can occur by the movement of dislocations on specific crystallographic slip systems. Each system comprises a slip plane and a slip direction within this plane. In practice, slip can occur on many different crystal systems. Furthermore, due to the trigonality of quartz, most slip systems have three alternative dispersion patterns and centres of rotation (e.g. Figs. 3b & c and 4b & c). The *combined* range of dispersion paths predicted for an individual slip system results in complex interconnected distributions consisting of small-/great-circle regions of relatively high frequencies, separated by regions of low/zero frequencies. The possibility perhaps exists for a crystal direction migrating along a dispersion path determined by one rotation centre, to switch to a related centre at the intersection of the respective pathways. This situation may allow significant increase in the migrational mobility of crystal directions and contribute to the development of preferred crystallographic orientations via the operation of a single crystal slip system in different directions.

Thus, for progressive rotational misorientation each slip system is characterized by specific relationships between the principal crystal directions involved. For example, basal-plane slip in the direction of **M3** produces subgrains and neoblasts with a coincident set of *a* axes parallel to **A2**; the *c* axes disperse along a great circle with **A2** as its pole and the remaining *a* and *m* poles disperse on small circles centred on **A2** (see Lloyd & Freeman 1991a). It is these relationships (summar-

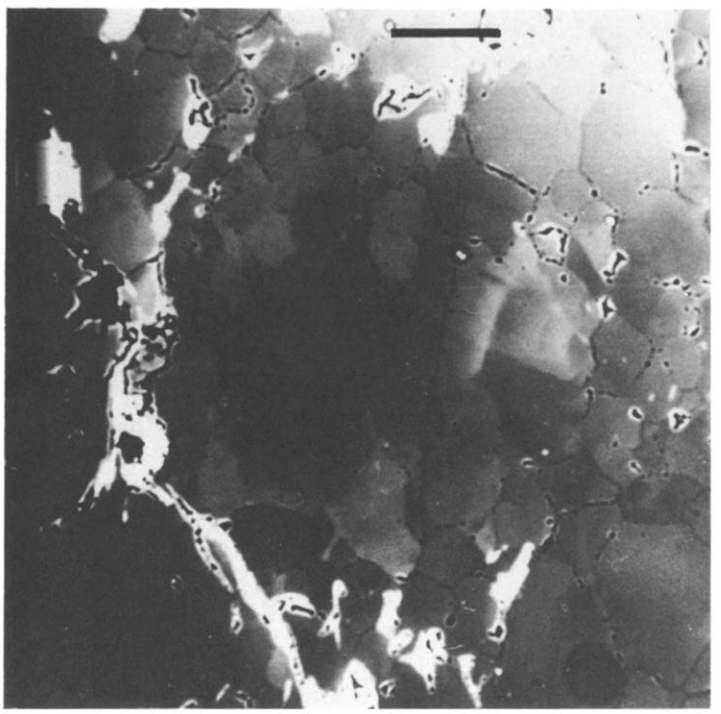

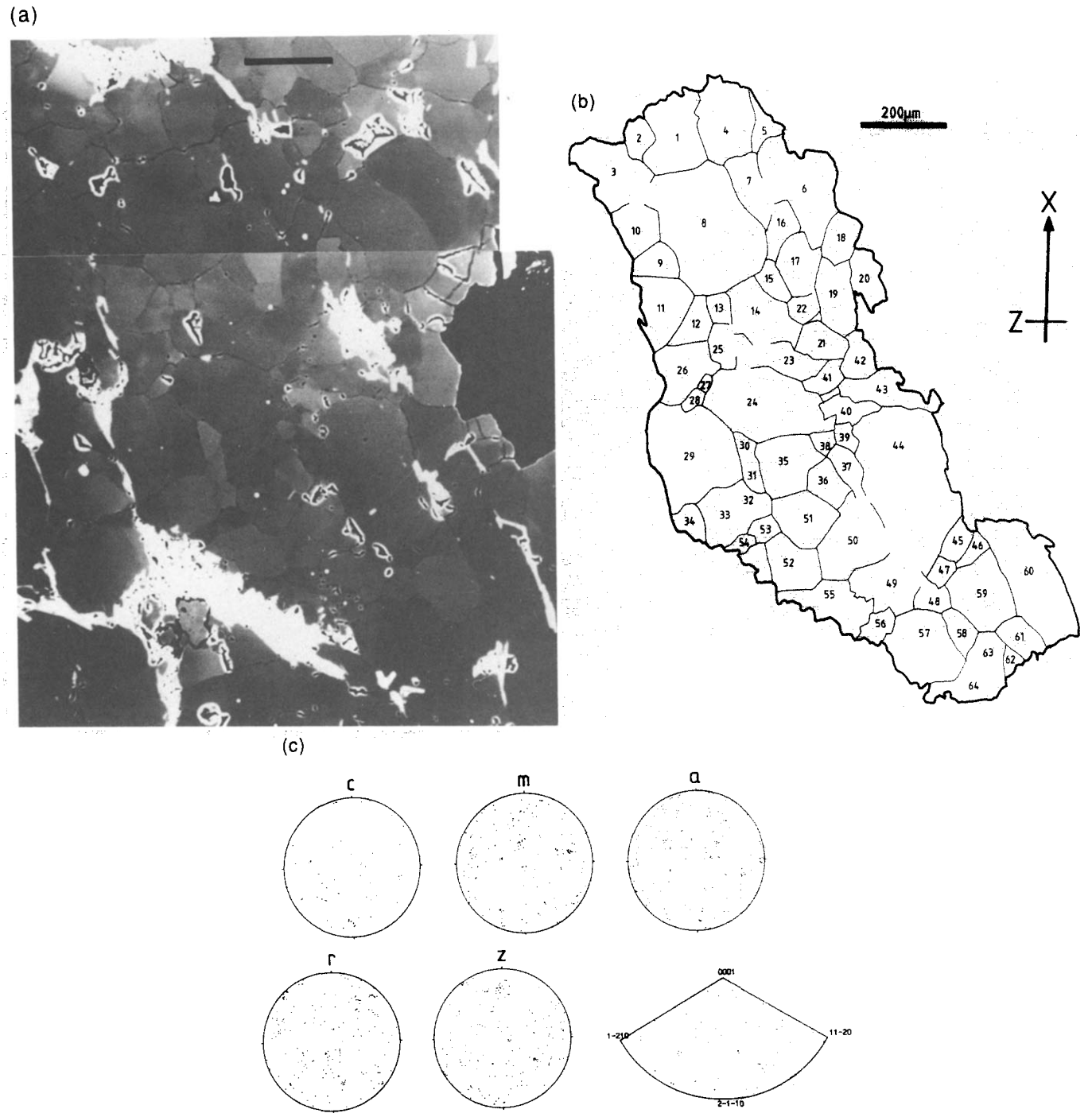

Fig. 2. Microstructural observations and crystallographic orientations determined via SEM–EC for Grain C (100% dynamically recrystallized). (a) SEM–EC orientation contrast image of porphyroclastic microstructure; scale bar 200 μm. (b) Schematic location map showing positions of neoblast grains (1–64) from which ECPs were obtained. (c) Individual orientation pole figures for the principal crystal directions *c*, *m*, *a*, *r* and *z* (*X*, east–west; *Z*, north–south; *Y*, vertical); see Table 2. Also shown is the inverse pole figure for the ECP/grain/specimen normal directions.

ized in Table 1) which are responsible for the development of distinctive crystal fabrics and microstructures. However, it should be emphasized that the dispersion patterns are not necessarily unique for a specific crystal slip system. For example, basal-plane slip accommodated in *equal*, alternate steps parallel to two adjacent *m* directions will produce exactly the dispersion patterns anticipated for basal-plane slip parallel to the intervening *a* axis. Nevertheless, we might expect this to be a unique situation and in general the alternating steps will probably involve unequal amounts of slip resulting in complex dispersion patterns, perhaps similar to those shown in Lloyd & Freeman (1991a, fig. 7).

Using the dispersion pattern approach, it is possible to establish whether a relationship exists between the dynamically recrystallized regions and the parent grain. This information can then be used to distinguish between rotational and migrational processes and to establish the dynamic recrystallization history for a particular porphyroclast.

PORPHYROCLAST DYNAMIC RECRYSTALLIZATION

Microstructural observations

(a) *Grain A*: 10–20% *dynamically recrystallized.* This grain (Fig. 1a) consists mostly of subgrains, although two distinct regions are distinguished: a central core region of rather diffuse orientation contrast and subgrain definition is surrounded by a mantle region of more pronounced and generally equant subgrains. SEM electron channelling patterns (ECP) from the core region are very distorted, indicating a high density of dislocations which have only partially coalesced to form distinctive subgrain walls. Accurate indexing of these patterns (i.e. numbers 46–67, Fig. 1b) proved difficult and they have been omitted from the analysis (e.g. Table 2). Variation in crystal orientation within this grain due to dynamic recrystallization is of minor significance and hence the original orientation of the parent grain is close to that of the mantle. We have obtained ECPs from 43 'subgrains' within the mantle (Fig. 1b), from which the principal crystal direction pole figures have been derived (Figs. 1c and 3a).

Just over half (23) of the subgrains have barely resolvable differences in orientation (summarized in Table 2), although there is an obvious slight dispersion (amounting to $\sim 5°$) away from the parent orientation (Fig. 1c). The positions of maximum frequency define a 'single crystal' (Fig. 3b), which almost certainly represents the orientation of the original parent porphyroclast grain (which we shall assume is defined exactly by ECP 30). The orientations of the remaining 21 subgrains appear to be rather remote from this origin and hence these should perhaps be referred to as neoblasts. However, many appear to be related to the parent orientation by strings of connected orientations (see also Table 2). This observation is central to our interpretation of the processes active during the dynamic recrystallization of this grain (see below).

(b) *Grain C*: 100% *dynamically recrystallized.* The texture of this originally porphyroclastic grain suggests that it is now totally replaced by much smaller neoblasts (Fig. 2a). Original subgrains are not obvious but many of the neoblasts contain distinct subgrain microstructures which probably represent subsequent dynamic recrystallization processes. However, only the determination of the crystal orientations of the neoblasts (and their subgrains) relative to the parent porphyroclast orientation can verify this textural interpretation.

We have obtained ECPs from 63 'neoblasts' (Fig. 2b) within the original porphyroclastic grain region (as defined by 'internal' rutile needle inclusion fabrics and 'external' mica grain-boundary decoration). Distributions of the principal crystal directions are dispersed (Figs. 2c and 4a), verifying the textural interpretation that the original porphyroclast now consists of many smaller neoblasts (*note*: subgrains within these neoblasts have orientations similar to each other and to their enclosing neoblast, but often very different from neighbouring neoblasts–neoblast-subgrains; this indicates that these are new generation subgrains, developed late in the dynamic recrystallization history after the development of the neoblast microstructure). The dispersed distributions make it difficult to recognize a reference orientation close to the original orientation of the parent porphyroclast, although several clusters of orientations do occur in each pole figure. The largest of the *c* clusters (comprising neoblasts 37–43, 53, 55 and 56) is also represented by clusters in the other pole figures. Thus, these neoblasts define an approximate 'single crystal' orientation (Fig. 4b). We shall therefore use this orientation (specifically ECP 40) to represent an internally consistent reference which allows comparison between all neoblast grains.

The simple systematics recognized in the crystal fabric of Grain A (and also Grain B of Lloyd & Freeman 1991a) are not immediately apparent in Grain C due to the larger rotations involved. Despite these large rotations, clusters of coincident orientations do occur. The criterion for deciding whether two directions are coincident is that their cones-of-error associated with initial measurement overlap (the error cone subtends an angle of $\sim 5°$). We can use this to show that the orientations in Grain C are non-random, as follows. Consider two adjacent grains with unknown, random orientations. There are nine opportunities for coincident *a* (or *m*, *r* or *z*) directions. Hence, the probability of observing a coincidence of *a* axes is $9\ E/A$, where E is the surface area of the hemisphere intersected by the cone-of-error, and A is the surface area of the entire hemisphere. In terms of Grain C, the probability of observing a coincidence is 0.04, whereas the observed coincidence is 0.18 (i.e. 4.5 times the random expectation). This clearly suggests that the crystal fabric of Grain C is also non-random.

Table 2. Coincidence relationships between parent, subgrains and neoblasts in Grains A (1–45) and C (1–64) determined via SEM ECP and *CHANNEL* analysis

GRAIN A														GRAIN C												
ECP	Crystal Directions													ECP	Crystal Directions											
	c	a 1	a 2	a 3	m 1	m 2	m 3	r 1	r 2	r 3	z 1	z 2	z 3		c	a 1	a 2	a 3	m 1	m 2	m 3	r 1	r 2	r 3	z 1	z 2	z 3
01			♦								t	t	T	01				o						o			
02			♦								t	t	T	02				♦				o	o	o	o	o	o
03			o			o		o	o	o				03				o			o						
04	♦	♦	♦	♦	♦	♦	♦	♦	♦	♦	♦	♦	♦	04		♦			o			o	o				
05	♦	♦	♦	♦	♦	♦	♦	♦	♦	♦	♦	♦	♦	05			o				o						
06	♦	♦	♦	♦	♦	♦	♦	♦	♦	♦	♦	♦	♦	06								t				o	
07	♦	♦	♦	♦	♦	♦	♦	♦	♦	♦	♦	♦	♦	07		o				o						o	
08	♦	♦	♦	♦	♦	♦	♦	♦	♦	♦	♦	♦	♦	08		o				o		t	t				
09	♦	♦	♦	♦	♦	♦	♦	♦	♦	♦	♦	♦	♦	09		o			o		o						
10	♦	♦	♦	♦	♦	♦	♦	♦	♦	♦	♦	♦	♦	10	o			o				o					
11	♦	♦	♦	♦	♦	♦	♦	♦	♦	♦	♦	♦	♦	11							o						
12				o			o				o	o	o	12		o			o			o					
13				o			o	t	t	t				13			o				o		o				
14		♦			o	o	o						t	14	o		o	o			♦			o			o
15		♦			o	o	o						t	15							o		o				t
16				o			o		o		t			16					♦				o				o
18	o		o	o	o	o	o	o			t			17		o								t	t	
19	♦	♦	♦	♦	♦	♦	♦	♦	♦	♦	♦	♦	♦	18		o								t	t	
20	♦	♦	♦	♦	♦	♦	♦	♦	♦	♦	♦	♦	♦	19		o								t	t	
21	♦	♦	♦	♦	♦	♦	♦	♦	♦	♦	♦	♦	♦	20				o	o			♦					
22			o								t	t		21		o								t	t		
23	♦	♦	♦	♦	♦	♦	♦	♦	♦	♦	♦	♦	♦	22	o		o	o			♦			o			o
24	♦	♦	♦	♦	♦	♦	♦	♦	♦	♦	♦	♦	♦	23	o		o	o			♦			o			o
25	♦	♦	♦	♦	♦	♦	♦	♦	♦	♦	♦	♦	♦	24							o		o		o		
26	♦	♦	♦	♦	♦	♦	♦	♦	♦	♦	♦	♦	♦	25			♦			o	o		o	o			
27	♦	♦	♦	♦	♦	♦	♦	♦	♦	♦	♦	♦	♦	26			o				o		o				
28	♦	♦	♦	♦	♦	♦	♦	♦	♦	♦	♦	♦	♦	27							♦			t			
29	♦	♦	♦	♦	♦	♦	♦	♦	♦	♦	♦	♦	♦	28			o			♦			o	o			
30	P	P	P	P	P	P	P	P	P	P	P	P	P	29			o			o			o	o			
31	♦	♦	♦	♦	♦	♦	♦	♦	♦	♦	♦	♦	♦	30							o	♦				o	
32	♦	♦	♦	♦	♦	♦	♦	♦	♦	♦	♦	♦	♦	31							o	♦				o	
33	♦	♦	♦	♦	♦	♦	♦	♦	♦	♦	♦	♦	♦	32							o	♦				o	
34		o		o			♦							33							o	♦				o	
35		o		o			♦							34			o			o					t	t	
36		o		o			♦							35							o						
37			♦								T	t		36	o	o	o		o	o	o					♦	
38					♦									37	♦	♦	♦	♦	♦	♦	♦	♦	♦	♦	♦	♦	♦
39					♦									38	♦	♦	♦	♦	♦	♦	♦	♦	♦	♦	♦	♦	♦
40	♦	♦	♦	♦	♦	♦	♦	♦	♦	♦	♦	♦	♦	39	♦	♦	♦	♦	♦	♦	♦	♦	♦	♦	♦	♦	♦
41				o		♦					T	t	t	40	P	P	P	P	P	P	P	P	P	P	P	P	P
43	o		o	o		o		o		o		♦		41	♦	♦	♦	♦	♦	♦	♦	♦	♦	♦	♦	♦	♦
44	o		o	o		o		o		o		♦		42	♦	♦	♦	♦	♦	♦	♦	♦	♦	♦	♦	♦	♦
45				o			o	♦	o	o		o		43	♦	♦	♦	♦	♦	♦	♦	♦	♦	♦	♦	♦	♦
														44		o					o			o	o	o	
														45				o	o					o	o	o	
														46				o	o					o	o	o	
														47							o	♦				o	
														48				♦					o	o	o	♦	o
														49				o	o			t	t	t			
														50						o				t			
														51								t		t			
														52	o	o			o	o	o	t				t	
														53	♦	♦	♦	♦	♦	♦	♦	♦	♦	♦	♦	♦	♦
														54													o
														55	♦	♦	♦	♦	♦	♦	♦	♦	♦	♦	♦	♦	♦
														56	♦	♦	♦	♦	♦	♦	♦	♦	♦	♦	♦	♦	♦
														58	o	♦	o		o	♦		t		t		o	
														59	o	♦			o	♦	o		o		t		
														60		o			o				t		o		
														61		o									o		
														62	o	♦	o		o	o		o	o			o	
														63													
														64													

KEY

P Inferred parent grain

♦ Coincident with parent grain

o Slightly displaced to parent grain

T twin relationship (*r* and/or *z*)

t displaced twin relationship (*r* and/or *z*)

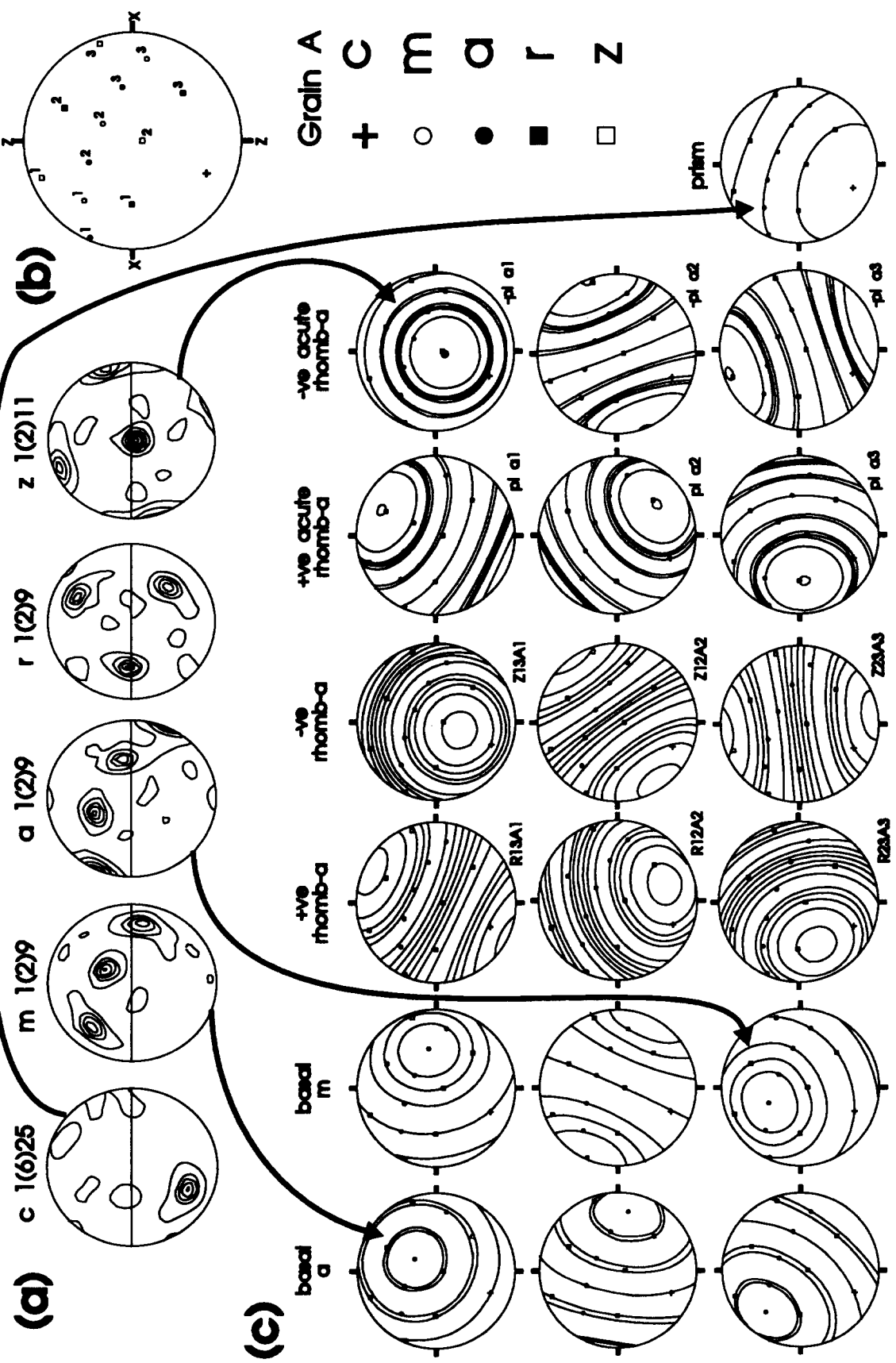

Fig. 3. Crystal direction dispersion patterns away from the interpreted original parent single crystal orientation for Grain A expected for crystal slip on specific systems. Comparison (connecting lines) suggests that basal-*a* slip dominated, with minor contributions from basal-*m* and basal-prism (*a* or *m*) slip. (a) Contoured (multiples of uniform distribution) pole figure diagrams showing the orientations of the principal crystal directions. Minimum (interval) maximum contour intervals as indicated; contouring procedure as for Lloyd & Freeman (1991a). (b) Approximate 'single crystal' orientation defined by the majority of subgrains–neoblasts. (c) The range of dispersion paths predicted for individual slip systems: basal-*a*, basal-*m*, basal-prism (*a* or *m*), rhomb-*a* (positive *r* and negative *z*), and acute (π) rhomb-*a* (positive *r* and negative *z*). Note that most systems have three alternative dispersion patterns due to the trigonality of quartz: C, *c*-axis; M1–3, three *m* directions; A1–3, three *a* axes; R1–3, three *r* directions; Z1–3, three *z* directions.

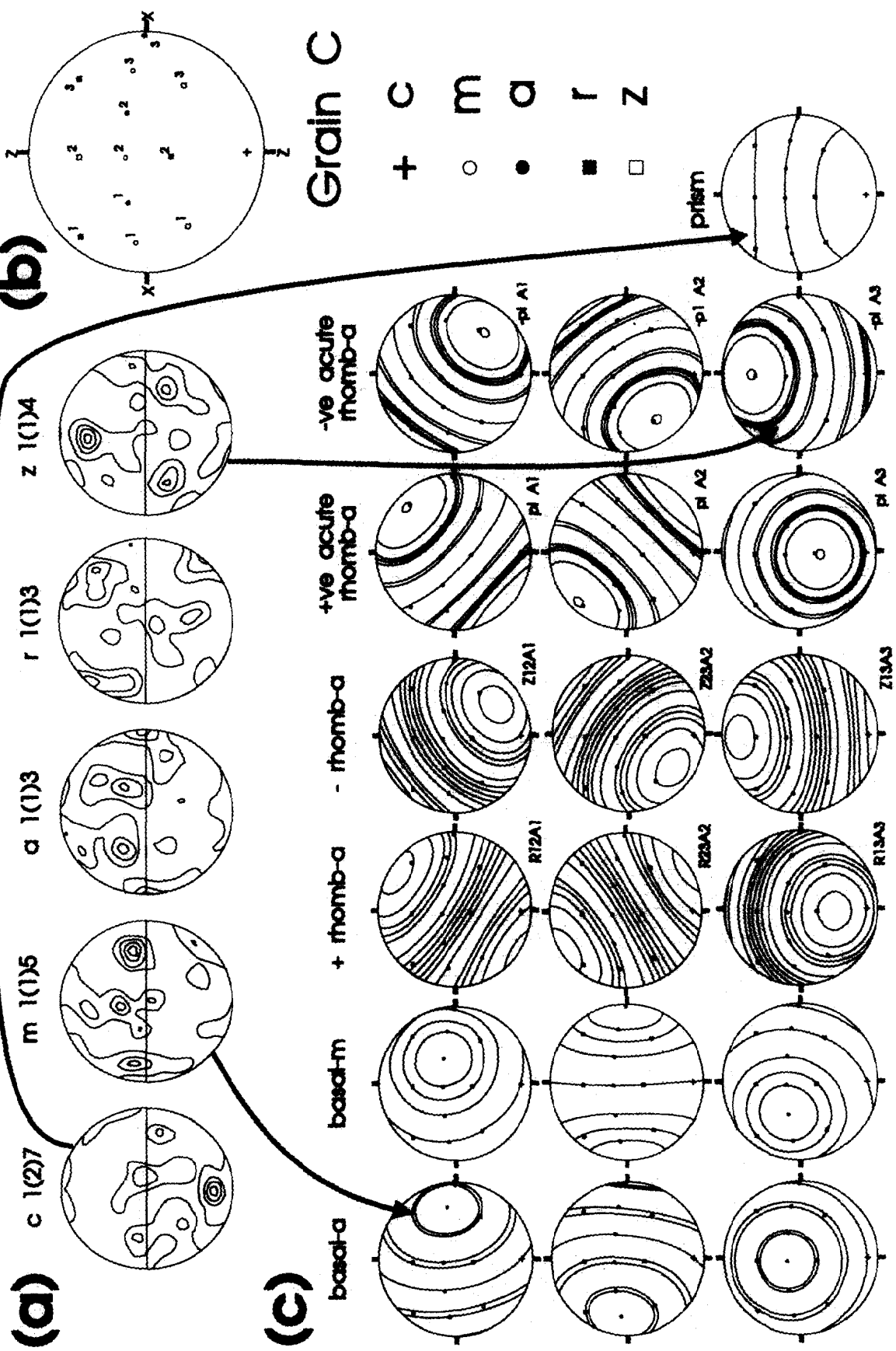

Fig. 4. Crystal direction dispersion patterns away from the interpreted original parent single crystal orientation for Grain C expected for crystal slip on specific systems. Comparison (connecting lines) suggests that basal-*a* slip dominated, with minor contributions from basal-*m* and basal-prism (*a* or *m*) slip. (a) Contoured pole figure diagrams. (b) Approximate 'single crystal' orientation defined by the majority of subgrains–neoblasts. (c) Range of dispersion paths predicted for individual slip systems. See caption to Fig. 3 for further details.

In fact, all but two (63 and 64) of the neoblasts examined have at least one crystal direction which is either coincident with, or only slightly dispersed from, the reference 'single crystal' orientation (summarized in Table 2). Furthermore, the large number of coincident crystal directions between the neoblasts and the 'single crystal' reference orientation (~50%) suggests that the latter actually represents the orientation of the original parent porphyroclast (Fig. 4b).

Recrystallization processes

(a) *Grain A*. In general, the crystal pole figures (Figs. 1c and 3a) show only slight dispersion from the original parent grain orientation (Fig. 3b). Four distinct clusters (**C**, **M2**, **A2** and **Z2**) can be recognized within the respective dispersion patterns, which suggests that these positions may have acted as rotation centres (Fig. 3c; see also Table 1). However, the dispersion trails of the principal directions away from the parent positions are almost wholly characteristic of basal-**A1** slip about the **M2** position and negative acute rhomb-**A1** slip about the **Z2** position. It is significant that the slip direction (**A1**) is not only the same for both systems but is also the direction close to the specimen *X* direction. Minor contributions (based on the relatively slight amounts of associated dispersion) from basal-**M3** slip about **A2** and 'basal prism' slip about **C** (although the specific slip direction cannot be determined) cannot be ruled out. The former is also characterized by a slip direction close to *X*, whereas the latter system could slip parallel to either **A1** and/or **M3**. Finally, a few subgrains (see Table 2) also show a transposition of some or all of their *r* and *z* directions in a manner typical of Dauphiné twinning (e.g. Lloyd *et al.* 1992, Mainprice *et al.* 1993).

Some 'subgrains' show large deviations of their crystal directions from the parent origin and we consider these to be neoblasts. They often have complex orientation relationships with the parent grain and probably developed via a combination of slip systems (see discussion of Grain B by Lloyd & Freeman 1991a). However, because parts of the boundary of Grain A proved difficult to define, it is possible that some of these neoblasts were not part of the original porphyroclast but developed (either by rotation or migration) from adjacent parent grains with different orientation characteristics.

Thus, the crystal direction dispersion patterns and relationships exhibited by Grain A are consistent with crystal slip and hence rotational dynamic recrystallization. This supports the suggestion made by Lloyd & Freeman (1991a), based on observations made on Grain B, that dynamic recrystallization under these temperature and strain rate conditions is initially dominated by subgrain rotation.

(b) *Grain C*. The large dispersion of the crystal direction distributions for this grain (Figs. 2c and 4a) makes interpretation of specific slip systems difficult. However, the statistically significant occurrence of neoblast crystal directions coincident with a 'single crystal' reference orientation (Fig. 4b) suggests that it should be possible to determine at least part of the dynamic recrystallization history. Indeed, comparison between the observed (Figs. 2c and 4a) and predicted (Fig. 4c) crystal direction distributions are surprisingly good given the potential complexity of the processes involved. The following dispersion patterns are recognized.

The crystal pole figures (Figs. 2c and 4a) include three distinct clusters (**C**, **M3** and **Z2**) within the respective dispersion patterns, parallel to the parent orientations (Fig. 4b), which suggests that these positions may have acted as rotation centres (Fig. 4c; see also Table 1). the **M3** cluster is responsible for much of the observed dispersion and is consistent with basal-**Al** slip. The **Z2** cluster is also responsible for significant dispersion and is consistent with negative acute rhomb-**A3** slip. Most of the remaining scatter in the pole figures can be explained by basal-prism slip about **C** (although the specific slip direction cannot be determined). In contrast to Grain A, there is little evidence for basal-*m* slip about any of the three *a* axes. The observed favoured slip directions are parallel to **A1** and **A3**. The latter is very close to the specimen *X* direction and perhaps constrains the basal-prism slip system to **<M2>(A3)**, although **<M3>(A1)** remains a possibility. A few subgrains (see Table 2) show a transposition of some or all of their *r* and *z* directions in a manner typical of Dauphiné twinning (e.g. Lloyd *et al.* 1992, Mainprice *et al.* 1993). This grain also contains an even greater number of anomalously large neoblasts than Grain B (compare Lloyd & Freeman 1991a, fig. 1). These neoblasts have long, straight boundaries terminating in 120° triple junctions (Figs. 2a & b) which indicate that significant, perhaps even post-kinematic, grain growth has occurred.

The crystal textures and coincidence relationships determined for Grain C are not too dissimilar from those recognized more clearly for Grain B mantle neoblasts (Lloyd & Freeman 1991a, figs. 5–8). We therefore conclude that the observed distributions and coincidences of crystallographic directions are again directly related to the dynamic recrystallization process(es). This leads us to make similar interpretations regarding the dynamic recrystallization history of Grain C. The recrystallization process initiated via crystal slip on a basal-*a* system. Although this system dominates the history, increasing misorientation requires additional slip systems to be activated (i.e. acute rhomb-*a* and basal-prism slip systems). However, the presence of numerous anomalously large neoblasts suggests that some or much of the initial rotational microstructure subsequently has been consumed by the growth of selected neoblasts involving grain-boundary migrational processes. It is not clear from the analysis whether the observed twin relationships are deformation or inherited features. Thus, although dynamic recrystallization initiated as a subgrain–grain rotational process (and significant recrystallization was achieved

Table 3. Predicted crystal slip systems recognized from pole figure dispersion patterns for Grains A and C (this study, e.g. Figs. 3 and 4), and Grain B (Lloyd & Freeman 1991a)

Crystal slip system		Grain A	Grain B	Grain C
Basal plane	-*a*1	Yes	Yes	Yes
	-*a*2	—	—	—
	-*a*3	—	Yes	—
Basal plane	-*m*1	—	Yes	—
	-*m*2	—	—	—
	-*m*3	Yes	Yes	
Prism planes	-*a*1	Yes	Yes	Yes
	-*a*2	—	—	—
	-*a*3	—	Yes	Yes
Prism planes	-*m*1	—	Yes	—
	-*m*2	—	—	—
	-*m*3	Yes	Yes	
Positive rhomb planes	-*a*1	—	—	—
	-*a*2	—	—	—
	-*a*3	—	—	
Negative rhomb planes	-*a*1	—	—	—
	-*a*2	—	—	—
	-*a*3	—	—	—
Positive acute rhomb planes	-*a*1	—	—	—
	-*a*2	—	Yes	—
	-*a*3	—	—	—
Negative acute rhomb planes	-*a*1	Yes	—	—
	-*a*2	—	—	—
	-*a*3	—	Yes	Yes

by this process), grain-boundary migration eventually becomes important.

DISCUSSION

Our SEM–EC observations (including those reported in Lloyd & Freeman 1991a) have recognized the following textural and fabric relationships in the dynamically recrystallized porphyroclasts of this greenschist facies Dalradian quartzite: (1) systematic variation in subgrain *c* direction orientations (e.g. mantle subgrains in Grain A, core subgrains in Grain B); (2) neoblasts which share a coincident *m* or *a* direction orientation and have only a small *c* direction misorientation with the parent grain (e.g. Grain A, Grain B group B2); (3) neoblasts which share a coincident *m* or *a* direction orientation and have a large *c* direction misorientation with the parent grain (e.g. Grain A, Grain B group B1a, b and Grain C); (4) neoblasts which share a coincident *c* direction orientation with the parent grain and whose *a* or *m* directions are distributed along the great circle defined by the basal plane to this grain (e.g. Grain B group B3); (5) neoblasts with neither coincident nor systematic *c* direction orientations or misorientations, but (local) coincidence of either *a*, *m* or *r*/*z* direction orientations (e.g. Grain C); and (6) transposition or *r* and *z* directions. We now use these relationships to suggest a composite dynamic recrystallization history for the quartz porphyroclasts in this representative specimen (see Fig. 5 and Table 3).

Our observations confirm the suggestion made by other workers (e.g. Hobbs 1968, Ransom 1971, Wilson 1973) that the dynamic recrystallization of an individual quartz porphyroclast (Fig. 5.1) is a sequential process involving both subgrain–grain rotation and grain-boundary migration. Dynamic recrystallization initiates as a subgrain rotation process via 'bending' of the parent grain on a single crystal slip system to form elongate polygonized subgrains, with a systematic orientation relationship between subgrains and parent (Fig. 5.2). This process can accommodate only small strains before subgrain rotation is activated; preserved polygonized subgrains are restricted to the least dynamically recrystallized parts of grains (e.g. Fig. 5.3; i.e. most of Grain A, core region of Grain B). Other grain regions, especially the mantle, continue to recrystallize due to rotation and crystal slip to form neoblasts (Fig. 5.4). To achieve large misorientations between neighbouring grain clusters requires more than one active slip system, but systematic orientation relationships between subgrains and/or neoblasts and their parent can still be recognized. Thus, whilst at first basal-*a* slip is sufficient to accommodate the misorientations (e.g. Grain A), eventually other systems (specifically basal-*m*, acute rhomb-*a* and basal-prism parallel to both *a* and *m*) need to be activated (e.g. Grain B).

Re-examination of Lloyd & Freeman's (1991a,b) crystal fabric data for Grain B reveals individual *r*

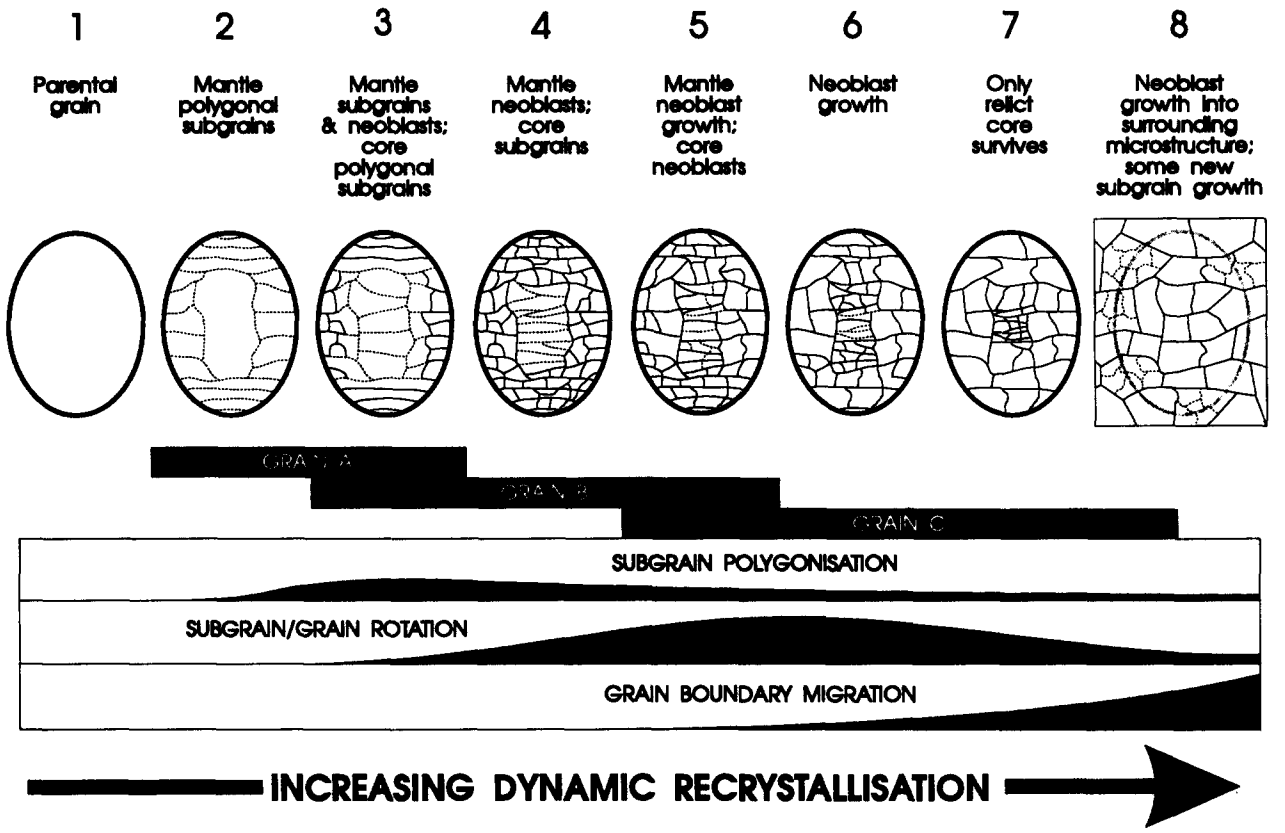

Fig. 5. Schematic summary of the dynamic recrystallization history of an individual porphyroclastic quartz grain determined by combining observations made on Grains A, B and C. The range of microstructures covered by each grain and the relative contributions of subgrain polygonization, subgrain rotation and grain boundary migration are also indicated. See text for details.

(subparallel to the Z specimen axis) and z direction clusters, indicative of acute rhomb-*a* crystal slip. This supports the suggestion of Law *et al.* (1990), based on observations on an amphibolite facies quartz mylonite, that acute rhomb-*a* slip is a potentially important slip system in quartz (see also Lloyd *et al.* 1992).

The rotational dynamic recrystallization microstructure produced by crystal slip (Fig. 5.4) is unlikely to be in equilibrium. The formation of (relatively) small subgrains and/or neoblasts produces locally high dislocation densities (i.e. in subgrain–neoblast boundary walls) and potentially large 'internal' strain energies. The resulting variations in dislocation density and strain energy distributions may be sufficient to initiate grain-boundary migration and the preferential growth of some neoblasts. Crystal slip also tends to produce straight subgrain and neoblast boundaries with orthogonal (i.e. 'T') triple point contacts. Such boundaries are perpendicular to the slip plane and the slip vector, an inherently unstable configuration prone to modification via boundary migration processes (e.g. *regime 3* of Hirth & Tullis 1992). The later stages of dynamic recrystallization (Figs. 5.5–5.7) are therefore characterized by the increasing significance of grain-boundary migration (e.g. Grains B and C). Eventually, migration must dominate and it overprints earlier microstructures, including those in adjacent grains (Fig. 5.8), to achieve equilibrium and stability. This behaviour is clearly shown in Table 3, where the number of crystal slip systems observed at first increases when subgrain–grain rotation processes dominate recrystallization (i.e. Grains A to B), and then decreases as migration processes takeover (i.e. Grains B to C). Furthermore, most of the observed crystal slip systems exploit the *a* slip direction(s) and any slip parallel to *m* systems which are recognized disappear as migrational processes take over the dynamic recrystallization (Table 3).

Our interpretation implies that Grains A, B and C represent stages of the same continuous history which is dependent principally on time–strain. The textural progression observed optically from other samples from the same major structure (the Kilmory Bay syncline), at different bulk strains, are similar to those discussed above. We therefore believe that the scheme outlined in Fig. 5 applies to most of the quartzites from this region. Intuitively, one would expect that initial orientation should also have a significant effect on the degree and mode of recrystallization. Our sample size is too small to test this idea. However, qualitatively, the basal planes for all three parent grains are oriented at moderate to high angles to the finite extension direction (see Figs. 3b and 4b) (see also Lloyd & Freeman 1991a, fig. 5). Assuming some correspondence between the orientation of the finite strain directions and the principal stresses, these basal planes would all support non-zero shear stresses and thus con-

stitute 'weak orientations'. With reference to the same rocks, Freeman (1985) concluded that the relatively strong grains (i.e. 'strong orientations') simply rotate in the finer grained matrix until the critical resolved shear stress (CRSS) passes through a threshold and activates a crystal slip system. In this respect, dynamic recrystallization probably does not begin until a grain has attained some weak orientation that is broadly equivalent for all grains. The key factor which permits this scheme of recrystallization to be so broadly applicable is the bimodal grain size and the subsequent partitioning of strain between the small and large grain size fractions. If the starting grain sizes had been unimodal, or constant, free rotation of porphyroclasts would be much less likely to occur. Deformation in *some* grains would then proceed on strong slip systems prior to the activation of weak slip systems in grains with strong orientations. In this case, our general scheme beginning with subgrain polygonization related to slip on a basal-*a* system should not hold.

CONCLUSIONS

(1) The SEM electron channelling technique has been used to identify the processes involved in the dynamic recrystallization of three quartz porphyroclasts (exhibiting 10–20, ~50 and 100% recrystallization, respectively) in a relatively pure quartzite deformed at low strains under greenschist facies conditions.

(2) Dynamic recrystallization of an individual quartz porphyroclast is a sequential process involving both subgrain–grain rotation and grain-boundary migration.

(3) Dynamic recrystallization initiates as a subgrain rotation process via crystal slip on a single system, leading to bending of the parent grain, elongate and polygonal subgrains, and a systematic orientation relationship between subgrains and parent.

(4) Continued subgrain, and subsequently neoblast, rotation requires more than one active slip system, although a systematic orientation relationship between subgrains–neoblasts and parent can still be recognized enabling the specific crystal slip systems to be identified.

(5) The specific crystal slip systems identified for the three grains are: basal-*a*, basal-*m*, acute rhomb-*a* and 'basal-prism' (parallel to either *a* and/or *m*). Dauphiné twinning was also recognized but its significance during dynamic recrystallization has yet to be determined.

(6) A dynamically recrystallized grain microstructure consisting of rotated subgrains and neoblasts is not necessarily stable and potentially large 'internal' strain energies may exist to drive grain-boundary migration and the preferential growth of some neoblasts during the later stages of dynamic recrystallization.

(7) The occurrence of new subgrains within migrational neoblasts suggests that dynamic recrystallization is a cyclical process which initiates via rotational processes but continues as a (varying) combination of subgrain–grain rotation and grain-boundary migration in an attempt to achieve microstructural equilibrium and/or stability.

(8) Grains A, B and C are typical of the porphyroclasts in this quartzite and represent different stages in the same continuous, time–strain-dependent, dynamic recrystallization history.

(9) The porphyroclasts have similar recrystallization histories because the original bimodal grain size distribution leads to strain partitioning between the small- and large-scale fractions, allowing the porphyroclasts to rotate into weak orientations with the subsequent activation of weak crystal slip systems.

Acknowledgements—We are grateful to the Journal's referees, Greg Hirth and Mark Jessell, for their constructive reviews which contributed to the final version of this manuscript. We have also benefited from discussions with Andy Farmer, Rob Knipe and Dave Mainprice. The SEM analyses were performed at Birmingham University with the help of Dr. Malcolm Hall and his 'spiral scanning' SEM/EC attachment. Niels-Henrik Schmidt is thanked for access to his ECP-indexing program *CHANNEL*.

REFERENCES

Avé L'Allement, H. G. 1978. Experimental deformation of diopside and websterite. *Tectonophysics* **48**, 1–27.

Bons, P. D. & Urai, J. L. 1992. Syndeformational grain growth: microstructures and kinetics. *J. Struct. Geol.* **14**, 1101–1109.

Cahn, R. W. 1965. *Physical Metallurgy*. North Holland, Amsterdam.

Cobbold, P. R., Means, W. D. & Bayly, M. B. 1984. Jumps in deformation gradients, and particle velocities across propagating coherent boundaries. *Tectonophysics* **108**, 283–298.

Drury, M. R., Humphreys, F. J. & White, S. H. 1985. Large strain deformation studies using polycrystalline magnesium as a rock analogue. Part II: dynamic recrystallisation mechanisms at high temperatures. *Phys. Earth & Planet. Interiors* **40**, 208–222.

Drury, M. R. & Urai, J. L. 1990. Deformation-related recrystallisation processes. *Tectonophysics* **172**, 235–253.

Etheridge, M. A. & Hobbs, B. E. 1974. Chemical and deformational controls on recrystallisation of mica. *Contr. Miner. Petrol.* **43**, 111–124.

Fitzgerald, J. D., Etheridge, M. A. & Vernon, R. H. 1983. Dynamic recrystallisation in a naturally deformed albite. *Textures & Microstruct.* **5**, 219–237.

Freeman, B. 1984. A method for quantitatively analysing dynamic recrystallisation in deformed quartzitic rocks. *J. Struct. Geol.* **6**, 655–662.

Freeman, B. 1985. Unpublished Ph.D. Thesis, University of Nottingham, U.K.

Garofalo, F., Zwell, L., Keh, A. S. & Weissmann, S. 1961. Substructure formation in iron during creep at 600°C. *Acta Metall.* **9**, 721–729.

Gifkins, R. C. 1976. Grain boundary sliding and its accommodation during creep and superplasticity. *Metall. Trans.* **7A**, 1225.

Guillope, M. & Poirier, J. P. 1979. Dynamic recrystallisation during creep of single crystalline halite: an experimental study. *J. geophys. Res.* **84**, 5557–5567.

Haessner, F. & Hoffman, S. 1978. Migration of high angle grain boundaries. In: *Recrystallisation of Metallic Materials* (edited by Haessner, F.). Rieder, Stuttgart, 63–95.

Hay, R. S. & Evans, B. 1988. Intergranular distribution of pore fluid and the nature of high-angle grain boundaries in limestone and marble. *J. geophys. Res.* **93**, 8959–8974.

Hirth, G. & Tullis, J. 1992. Dislocation creep regimes in quartz aggregates. *J. Struct. Geol.* **14**, 145–159.

Hobbs, B. E. 1968. Recrystallisation of single crystals of quartz. *Tectonophysics* **6**, 353–401.

Jessell, M. W. 1986. Grain-boundary migration and fabric develop-

ment in experimentally deformed octachloropropane. *J. Struct Geol.* **8**, 527–542.

Joesten, R. 1983. Grain growth and grain-boundary diffusion in quartz from the Christmas Mountain (Texas) contact aureole. *Am. J. Sci.* **283A**, 233–254.

Joy, D. C., Newbury, D. E. & Davidson, D. L. 1982. Electron channelling patterns in the scanning electron microscope. *J. Appl. Phys.* **53**, R81–R122.

Kerrich, R., Beckinsale, R. D. & Durham, J. J. 1977. The transition between deformation regimes dominated by intercrystalline diffusion and intercrystalline creep evaluated by oxygen isotope thermometry. *Tectonophysics* **38**, 241–257.

Law, R. D., Schmid, S. M. & Wheeler, J. 1990. Simple shear deformation and quartz crystallographic fabrics: a possible natural example from the Torridon area of NW Scotland. *J. Struct. Geol.* **12**, 29–46.

Lloyd, G. E. 1983. Strain analysis using the shape of expected and observed continuous frequency distributions. *J. Struct. Geol.* **5**, 225–231.

Lloyd, G. E. 1987. Atomic number and crystallographic contrast images with the SEM: a review of backscattered electron techniques. *Mineral. Mag.* **51**, 3–19.

Lloyd, G. E. & Freeman, B. 1991a. SEM electron channelling analysis of dynamic recrystallisation in a quartz grain. *J. Struct. Geol.* **13**, 945–953.

Lloyd, G. E. & Freeman, B. 1991b. Dynamic recrystallization of a quartz porphyroclast. Proceedings "International Conference on Textures of Materials 9", Avignon, France (1990). *Textures & Microstruct.* **14–18**, 751–756.

Lloyd, G. E., Law, R. D., Mainprice, D. & Wheeler, J. 1992. Microstructural and crystal fabric evolution during shear zone formation. *J. Struct. Geol.* **14**, 1079–1100.

Lloyd, G. E., Schmidt, N.-H., Mainprice, D. & Prior, D. J. 1991. Crystallographic textures. *Mineral. Mag.* **55**, 331–345.

Mainprice, D., Lloyd, G. E. & Casey, M. 1993. Individual orientation measurements in quartz polycrystals: advantages and limitations for texture and petrophysical property determinations. *J. Struct. Geol.* **15**, 1169–1187.

McLaren, A. C. 1986. Some speculations on the nature of high-angle grain boundaries in quartz rocks. In: *Mineral and Rock Deformation: Laboratory Studies—The Paterson Volume* (edited by Hobbs, B. E. & Heard, H. C.). *Am. Geophys. Un. Geophys. Monogr.* **36**, 233–247.

McClay, K. R. & Atkinson, B. K. 1977. Experimentally induced kinking and annealing of single crystals of galena. *Tectonophysics* **39**, 175–193.

Means, W. D. 1983. Microstructure and micromotion in recrystallisation flow of octachloropropane: a first look. *Geol. Rdsch.* **72**, 511–528.

Means, W. D. 1989. Synkinematic microscopy of transparent polycrystals. *J. Struct. Geol.* **11**, 163–174.

Means, W. D. & Jessell, M. W. 1986. Accommodation migration of grain boundaries. *Tectonophysics* **127**, 67–86.

Means, W. D. & Ree, J. H. 1988. Seven types of subgrain boundaries in octachloropropane. *J. Struct. Geol.* **10**, 765–770.

Ohtomo, M. & Wakahama, G. 1982. Crystallographic orientation of recrystallised grain in strained single crystal of ice. *Low Temp. Sci. Ser. A* **41**, 1–9.

Ohtomo, M. & Wakahama, G. 1983. Growth-rate of recrystallisation in ice. *J. Phys. Chem.* **87**, 4139–4142.

Poirier, J.-P. & Guillope, M. 1979. Deformation induced recrystallisation of minerals. *Bull. Mineral.* **102**, 67–74.

Poirier, J.-P. & Nicolas, A. 1975. Deformation-induced recrystallisation due to progressive misorientation of subgrains, with special reference to mantle peridotites. *J. Geol.* **83**, 707–720.

Ransom, D. M. 1971. Host control of recrystallised quartz grains. *Mineral. Mag.* **38**, 83–88.

Roberts, J. L. 1977. The Dalradian rocks of Knapdale and N. Kintyre. *Scott. J. Geol.* **13**, 113–124.

Schmidt, N.-H. & Olesen, N. O. 1989. Computer-aided determination of crystal lattice orientation from electron channelling patterns in the SEM. *Can. Mineral.* **27**, 15–22.

Toriumi, M. 1982. Grain-boundary migration in olivine at atmospheric pressure. *Phys. Earth & Planet. Interiors* **30**, 26–35.

Tullis, J., Christie, J. M. & Griggs, D. T. 1973. Microstructures and preferred orientations of experimentally deformed quartzites. *Bull. geol. Soc. Am.* **84**, 297–314.

Urai, J. L. 1983. Water assisted dynamic recrystallisation and weakening in polycrystalline bischofite. *Tectonophysics* **96**, 125–127.

Urai, J. L. 1985. Water-enhanced dynamic recrystallisation and solution transfer in experimentally deformed carnallite. *Tectonophysics* **120**, 285–317.

Urai, J. L., Means, W. D. & Lister, G. S. 1986. Dynamic recrystallisation of minerals. In: *Mineral and Rock Deformation: Laboratory Studies—The Paterson Volume* (edited by Hobbs, B. E. & Heard, H. C.). *Am. Geophys. Un. Geophys. Monogr.* **36**, 161–199.

Vernon, R. H. 1975. Deformation and recrystallisation of a plagioclase grain. *Am. Mineral.* **60**, 884–888.

Vernon, R. H. 1981. Optical microstructure of partly recrystallised calcite in some naturally deformed marbles. *Tectonophysics* **78**, 601–612.

Wenk, H.-R. & Christie, J. M. 1991. Comments on the interpretation of deformation textures in rocks. *J. Struct. Geol.* **13**, 1091–1110.

White, J. C. & White, S. H. 1981. On the structures of grain boundaries in tectonites. *Tectonophysics* **78**, 613–628.

White, S. H. 1976. The effects of strain on the microstructures, fabrics and deformation mechanisms in quartz. *Phil. Trans. R. Soc. Lond.* **A283**, 69–86.

Wilson, C. J. L. 1973. The prograde microfabric in a deformed quartzite sequence, Mount Isa, Australia. *Tectonophysics* **19**, 39–81.